Physics – Uspekhi **62** (11) 1153 – 1161 (2019)

CONFERENCES AND SYMPOSIA

PACS numbers: **04.30. – w**, 97.60.Lf

Spins of black holes in coalescing compact binaries

K A Postnov, A G Kuranov, N A Mitichkin

DOI: https://doi.org/10.3367/UFNe.2019.04.038593

Contents

Abstract. Modern astrophysical methods for determining spins of rotating stellar-mass black holes in close binaries and of supermassive black holes in active galactic nuclei are briefly discussed. Effective spins of coalescing binary black holes derived from LIGO/Virgo gravitational wave observations are specially addressed. The effective spins of coalescing astrophysical binary black holes and black holes with neutron stars are calculated for two plausible models of black hole formation from stellar core collapses (without or with an additional fallback from the stellar envelope) taking the stellar metallicity and star formation rate evolution in the Universe into account. The calculated distributions are consistent with the reported LIGO/Virgo observations. Distributions of the effective spins expected in yet undiscovered neutron star – black hole binaries have been calculated. The effective spins of primordial coalescing stellar-mass black holes can reach a few percent due to the accretion spin-up in a cold external medium.

Keywords: gravitational waves, black holes

1. Introduction

1.1 The Kerr metric

In Einstein's general relativity (GR), the structure of space–time around a stationary rotating black hole (BH) in a vacuum is fully described by the axially symmetric steady Kerr metric [1]. The parameters of the metric include the BH mass M and angular momentum J, which can be conveniently expressed in dimensional angular momentum units $a = J/(GM/c)$. In the Boyer–Lindquist coordinates [2] minimizing the number of nondiagonal metric elements, the Kerr metric can be written in the form [1]

$$\begin{aligned} \mathrm{d}s^2 &= -\left(1-\frac{2Mr}{\Sigma}\right)\mathrm{d}t^2 - \frac{4Mar\sin^2\theta}{\Sigma}\,\mathrm{d}t\,\mathrm{d}\phi + \frac{\Sigma}{\Delta}\,\mathrm{d}r^2 \\ &\quad + \Sigma\,\mathrm{d}\theta^2 + \left(r^2+a^2+\frac{2Ma^2r\sin^2\theta}{\Sigma}\right)\sin^2\theta\,\mathrm{d}\phi^2\,, \\ \Delta &\equiv r^2 - 2Mr + a^2\,, \quad \Sigma \equiv r^2 + a^2\cos^2\theta\,. \end{aligned} \tag{1}$$

The richness of the mathematical structure and physical effects in the Kerr metric is described in dedicated texts (see, e.g., [3]). The condition for the presence of a horizon ($g_{rr} \to \infty$) and the absence of a 'naked' singularity in a rotating BH requires $-M \leqslant a \leqslant M$. Measuring the mass in units of the BH mass M renders the Kerr parameter a dimensionless, $|a^*| \leqslant 1$. Below, we use the dimensionless parameter a^* and call it the 'BH spin'.

As $|a| \to 0$, Kerr metric (1) transforms into the Schwarzschild metric, and at large distances the Kerr metric *asymptotically* [2] turns into the metric for a steadily rotating body in a vacuum that was derived from Einstein equations in the weak-field limit in 1918 by Lense and Thirring [4]. From the astrophysical standpoint, any celestial body rotates and therefore the collapse of massive stars should generally result in the formation of rotating BHs with a nonzero parameter a.

An important notion we use below is the last marginally stable orbit of test particles (or innermost stable circular orbit, ISCO) in the Kerr metric. These orbits determine the inner boundary of an accretion disc around a rotating BH and are probed by astrophysical observations. In the equatorial plane $\theta = \pi/2$, the ISCO radius r_{ISCO} depends on the BH

K A Postnov [1, 2, 3, *], **A G Kuranov** [1, 4], **N A Mitichkin** [1, 2]
[1] Lomonosov Moscow State University,
Sternberg Astronomical Institute,
Universitetskii prosp. 13, 119234 Moscow, Russian Federation
[2] Lomonosov Moscow State University, Faculty of Physics,
Leninskie gory 1, 119991 Moscow, Russian Federation
[3] Novosibirsk State University, Department of Physics,
ul. Pirogova 2, 630090 Novosibirsk, Russian Federation
[4] All-Russian Academy of International Trade,
ul. Pudovkina 4a, 119285 Moscow, Russian Federation
E-mail: [*] kpostnov@gmail.com

Received 13 June 2019
Uspekhi Fizicheskikh Nauk **189** (11) 1230 – 1239 (2019)
DOI: https://doi.org/10.3367/UFNr.2019.04.038593
Translated by K A Postnov; edited by A M Semikhatov

[1] Here, we use geometrical units $G = c = 1$, unless stated otherwise.

[2] We note that the space–time around a nonrotating spherically symmetric body in a vacuum is exactly described by the Schwarzschild metric (Birkhoff's theorem).

spin a: for a Schwarzschild BH ($a = 0$), $r_{\rm ISCO} = 6M = 3r_{\rm g}$ (the gravitational radius is $r_{\rm g} = 2M \simeq 3$ km $(M/M_\odot)$) [6]. For $a > 0$, i.e., in the case of corotating particles, the ISCO radius decreases as $r_{\rm ISCO} \approx 3r_{\rm g} - (4\sqrt{6}/3)a$ for $a \ll M$, and in the case $a = M(1-\delta)$ with $\delta \ll 1$ approaches $r_{\rm ISCO} \simeq (r_{\rm g}/2)(1 + (4\delta)^{1/3})$, being above the outer BH horizon $r_+ \approx (r_{\rm g}/2)(1 + (2\delta)^{1/2})$ [7]. For example, for an accretion disc in a close binary system or in a galactic nucleus, $a \approx 0.9981$ (the Thorne limit determined by the balance of the angular momentum of an accreting BH in the photon field of the disc) [8], and the ISCO radius is $r_{\rm ISCO}(0.998) \approx 1.23M$.

Thus, both the mass M and the spin a^* of a BH are the most important parameters that can be measured or estimated from astrophysical observations. These observations are different for stellar-mass BHs $\sim (3-60)M_\odot$ in close binaries and supermassive BHs (SMBHs) with $M > 10^6 M_\odot$ in galactic nuclei.

Methods of BH parameter estimations from astronomical observations have been extensively discussed in the literature (see, e.g., reviews [9, 10] and the references therein). The most reliable mass estimates of stellar-mass BHs are obtained from dynamical measurements of the motion of the secondary companion (optical star) in close binary systems (CBSs). Orbits in such systems are almost circular. In this case, the radial velocity amplitude measured from spectroscopic observations $K_{\rm v} = V_{\rm v} \sin i$ (i is the binary orbit inclination, the angle between the orbital angular momentum and the line of sight) and the binary orbital period $P_{\rm b}$ enable the construction, using formulas of the classical two-body problem, of a combination with the dimension of mass, the so-called 'mass function' of the invisible component with a mass $M_{\rm x}$, which for a circular orbit is given by

$$f(M_{\rm x}) = \frac{K_{\rm v}^3 P_{\rm b}}{2\pi G} = \frac{M_{\rm x} \sin^3 i}{(1+q)^2}\,, \qquad (2)$$

where $q = M_{\rm v}/M_{\rm x}$ is the mass ratio of the visible to the invisible component of the binary. Clearly, the mass function sets only a lower mass limit of the unseen component, because the determination of the orbital binary inclination requires independent measurements.[3] It is accepted to consider the condition $M_{\rm x} \gtrsim 3M_\odot$ for the mass of the unseen component in a CBS as the necessary signature of a BH [12, 13]. This mass limit of the unseen relativistic component without evidence of a solid surface is attained in two dozen close X-ray binaries [10, 14].

The advent of gravitational-wave (GW) astronomy [15] offered a novel possibility to estimate the masses and spins of BH components in coalescing binary systems observed by LIGO/Virgo GW interferometers [16–18].

1.2 Black hole spins in X-ray binaries and galactic nuclei

Measuring BH spins is a much more difficult task than measuring BH masses and is model-dependent. In X-ray binaries, the matter from the gravitationally captured stellar wind of the optical star of early spectral class (e.g., in Cyg X-1) or from the Roche lobe overflow by an optical star (e.g., in GRS 1915+105, A0620-00, etc.) forms an accretion disc around the BH. The viscous friction in the differentially rotating disc heats the gas to very high temperatures, and the matter loses its angular momentum and gradually diffuses in the thermal time scale towards the BH. The inner radius of the accretion disc is determined by the ISCO around the BH, $r_{\rm ISCO}$: particles in the region $r < r_{\rm ISCO}$ freely fall into the BH. The structure and properties of stationary accretion discs around BHs are determined by the mass accretion rate $\dot{M}$ through the disc, physical parameters of the gas (radiation opacity, viscosity coefficient, etc.), and by the boundary conditions at the inner radius [19–22].

Thus, measurements of spectral and time characteristics of the emission from accretion discs around BHs enables indirect estimates of their masses and spins. A modern review of such observations and the list of sources can be found in [23].

The spin of BHs in X-ray binaries and galactic nuclei can be estimated in different ways (see [24] for a recent review and critical comments in [25]).

1.2.1 Continuum spectrum of the accretion disc. Through the boundary condition at the inner disc radius, the BH spin affects the form of the thermal spectral continuum radiated by the accretion disc. But the large number of model parameters (the accretion disc type, the BH mass, the distance to the source, the viewing angle, parameters of the hot corona above the disc, etc.) does not allow precise measurements of BH spins (see Table 2 in [23] for X-ray binaries).

1.2.2 Fluorescent iron line spectroscopy. Spins of accreting BHs can also be estimated from the spectroscopy of the K_α iron line (at energies from 6.4 keV for neutral iron to 6.9 keV for hydrogen-like iron Fe XXVI). This line emerges during the reflection of hard X-ray emission that can be generated in a hot scattering corona above the disc from a relatively cold gas in the inner parts of the disc ($< 10^7$ K) [26]. The reflected line has an equivalent width of ~ 150 eV. Due to relativistic effects at the inner disc radius, the line profile is red-shifted and acquires a width of ~ 1 keV [27]. Depending on the viewing angle and the assumed emission model, the blue wing of the line sharply drops at the gravitationally red-shifted frequency. The fluorescent iron line from the inner parts of an accretion disc around an SMBH was first observed in the galaxy MCG-6-30-15 [28]. For SMBHs in galactic nuclei, determining the spin from K_α iron line spectroscopy is the only means available (other than direct EHT observations of the BH shadow in the nucleus of the M87 galaxy; see Section 1.2.4 below). The profiles of the fluorescent K_α and L_α iron lines have been accurately measured in the spectra of several sources, in particular, in the Seyfert galaxy 1H0707-495 [29]. (The list of SMBHs with spins calculated by iron line spectroscopy can be found, for example, in Table 3 in [23]). Unlike continuum spectral fitting, the analysis of the fluorescent iron line profile formed by the reflection from the disc does not require knowledge of the BH mass, the distance to the source, or the disc inclination angle to the observer. We note that both methods yield consistent estimates of the parameter a^* for accreting BHs in X-ray binaries (see Table 2 in [23]).

1.2.3 X-ray quasiperiodic oscillations (QPOs). Observations of quasiperiodic oscillations of X-ray flux offer yet another method to estimate spins of accreting BHs [30]. In BH sources, QPOs have been observed at different frequencies,

[3] The binary orbit inclination cannot be obtained from spectroscopic measurements using Newtonian dynamics. However, this becomes possible in very close binaries with neutron stars (pulsars) using relativistic effects [11].

including low-frequency QPOs (from fractions of Hz to dozens of Hz) and high-frequency QPOs (several hundred Hz). High-frequency QPOs are close to some characteristic oscillations for stellar-mass BHs: the Keplerian frequency $f_{\rm K}$ and the radial $f_{\rm r} \sim f_{\rm K}$ and vertical $f_\theta \sim f_{\rm K}$ epicyclic frequencies [31, 32]:

$$f_{\rm K}(r) \simeq 220\ {\rm Hz} \left(\frac{10M_\odot}{M}\right)\left(\frac{6M}{r}\right)^{3/2}\left[1 \pm a^*\left(\frac{M}{r}\right)^{3/2}\right]^{-1}. \quad (3)$$

Applying this model to X-ray QPOs observed by the RXTE (Rossi X-ray Timing Explorer) observatory enabled high-precision estimations of masses and spins of BHs in GRO J1655-40 ($M = (5.31 \pm 0.07)M_\odot$, $a^* = 0.290 \pm 0.003$) [33] and XTE J1550-564 ($a^* = 0.34 \pm 0.01$), which coincided with spectroscopic estimates. We also note that the observed spectral correlations of X-ray QPOs in accreting BHs can be used for independent measurements of BH masses [35].

1.2.4 Observations of an SMBH in M87 by the Event Horizon Telescope (EHT). Recently, the first results of 1.3 mm VLBI observations of an SMBH in the active nucleus of the M87 galaxy ($M = (6.5 \pm 0.7) \times 10^9 M_\odot$) with a record high angular 10-microarcsec resolution carried out by EHT dishes have been reported [36]. Relativistic MHD modeling of the observed asymmetric radio brightness in the visible 'photon ring' from optically thin hot plasma around this SMBH, with the relativistic effects of photon propagation in gravitational field of a Kerr BH taken into account, enabled the BH spin estimate $a^* \approx 0.5$ or $a^* \simeq 0.94$ [37]. We note that models with a Schwarzschild BH are rejected by these observations as well as by the presence of a relativistic jet from the M87 nucleus with a power $P_{\rm j} \lesssim 10^{42}$ erg s^{-1}. An independent estimate of the BH spin in M87, $a^* = 0.9 \pm 0.1$, was also obtained in [38] from an analysis of the 'twisted light' in the Kerr metric.

Thus, observations of accreting BHs in X-ray binaries and galactic nuclei suggest fairly high spins of these BHs. This is apparently related to a prolonged accretion of matter and the history of SMBH mass growth in galactic nuclei in the course of galactic mergings.

2. Spins of coalescing binary black holes

2.1 Effective spins from LIGO/Virgo observations

LIGO/Virgo observations of coalescing binary BHs [16] provide new independent information on the masses and spins of coalescing binary BHs. In the quadrupole approximation, the form and amplitude of the GW signal from inspiraling compact objects are determined by a combination of masses M_1 and M_2 called the chirp mass: $\mathcal{M} \equiv (M_1 M_2)^{3/5}/M^{1/5} = M_1[q^2(1+q)]^{-1/5}$, where $q = M_1/M_2$ is the binary mass ratio and $M = M_1 + M_2$ is the total mass of the binary system. The chirp mass is the most precise parameter that can be determined from GW observations (see [16]). Spins of the components of a coalescing binary system are much more difficult to estimate. However, analyzing the form of the inspiraling GW signal enables measuring the so-called 'effective spin' of the coalescing binary, a mass-weighted combination of spin projections of the components on the orbital angular momentum:

$$\chi_{\rm eff} = \frac{M_1 a_1^* \cos\theta_1 + M_2 a_2^* \cos\theta_2}{M}, \quad (4)$$

where θ_i is the angle between the ith-component spin and the binary orbital angular momentum.

Most of the detected LIGO/Virgo binary BHs (except two sources, GW151226 and GW170729) have been found to have near-zero effective spin (within measurement errors) [16]. At first glance, this fact seems unusual because collapsing massive stars should have rotating cores [39] leading to the formation of BHs with nonzero spins. Rapidly rotating BHs from stellar core collapses have been thought to be 'central engines' generating narrow-beamed relativistic jets observed as long gamma-ray bursts [40]. Therefore, it would be interesting to understand whether it is possible to obtain close to zero effective spins of coalescing binary BHs formed in the standard astrophysical evolutionary channel from massive binary field stars [41–43].

2.2 Model assumptions

It is difficult to measure the rotation of stellar cores from observations. The theory of the evolution of rotating stars involves many parameters to describe the stellar core rotation, including the hypothesis about core–envelope coupling by the internal magnetic field [44], internal inertial gravitational waves [45], and other physical mechanisms of angular momentum transport (see [39] for more details). To describe the complicated evolution of the core of a massive star, a semi-phenomenological approach was suggested in [46], where the star was split into two parts, the core and the envelope, whose coupling was described by one effective parameter, the characteristic time of the angular momentum transfer $\tau_{\rm c}$. In this two-zone model, the change in the angular momentum of the core is written as

$$\frac{{\rm d}\mathbf{J}_{\rm c}}{{\rm d}t} = -\frac{I_{\rm c} I_{\rm e}}{I_{\rm c} + I_{\rm e}} \frac{\mathbf{\Omega}_{\rm c} - \mathbf{\Omega}_{\rm e}}{\tau_{\rm c}}, \quad (5)$$

where $I_{\rm c}$, $\Omega_{\rm c}$ and $I_{\rm e}$, $\Omega_{\rm e}$ are the moments of inertia and angular rotational velocities of the core and the envelope. It was shown in [46] that to describe the distribution of rotation periods of young pulsars derived from observations, the characteristic coupling time should be of the order of $\tau_{\rm c} \simeq 5 \times 10^5 - 10^6$ years, i.e., should approximately coincide with the evolutionary time of a massive star after the main sequence.

If a BH is born in a massive binary system, the rotation of the stellar core prior to collapse is also affected by the tidal coupling between the stellar envelope and the orbital motion of the secondary component. Taking the results obtained in [46] into account, the results of calculations of the effective spins of coalescing binary BHs were presented in [47] for different formation channels with account of both the metallicity and star formation history (dependence of redshift) in galaxies. These calculations adopted the standard theory of evolution of massive close binaries [42] in addition to the treatment of the rotational evolution of stellar cores using the coupling in (5). The key unknown element of double BH formation from massive binaries is the common envelope (CE) stage. This stage has been treated using the efficiency parameter $\alpha_{\rm CE}$, which is the fraction of the orbital energy transferred to the stellar envelope during the binary inspiral inside the common envelope: $\Delta E_{\rm env} = \alpha_{\rm CE} \Delta E_{\rm orb}$, where $E_{\rm env}$ is the binding energy of the envelope in the stellar core [48, 49].

The poorly known physics of BH formation at the end of a massive star evolution was parameterized by two models. In the first model, the entire stellar C–O core formed after a main sequence star collapsed into a BH, $M_{\rm BH} = 0.9 M_{\rm CO}$

(taking a 10% gravitational mass defect into account), and hence the total mass of a binary BH was $M = 0.9(M_{\rm CO,1} + M_{\rm CO,2})$. The BH angular momentum in this model was set equal to that of the C–O core: $J_{\rm BH} = J_{\rm CO}$.

In the second model, part of the stellar envelope above the C–O core $\Delta M_{\rm fb}$ was assumed to fall back onto a BH collapsed from the iron core $M_{\rm Fe}$ (the fallback model); the BH mass was calculated as in [50]. Thus, in this model, the BH mass was $M_{\rm BH} = 0.9(M_{\rm Fe} + \Delta M_{\rm fb})$ with $\Delta M_{\rm fb} = \max(M_{\rm BH} - 0.9M_{\rm CO}, 0)$. The BH angular momentum, which changes due to the fallback from the rotating envelope, is $J_{\rm BH} = J_{\rm CO} + \Delta J_{\rm fb}$, where $\Delta J_{\rm fb} = j_{\rm fb}\Delta M_{\rm fb}$. The specific angular momentum of the rotating envelope matter accreting onto the BH was assumed to be $j_{\rm fb} = \delta M_{\rm BH}$ with the coefficient $\delta = 2$ (the mean value between the specific angular momentum of particles on the ISCO around a Schwarzschild BH, $\delta = 2\sqrt{3}$, and around an extreme Kerr BH, $\delta = 2/\sqrt{3}$).

To calculate the effective spin of coalescing BHs, the angle between the BH spin vector and the orbital angular momentum should be specified (see Eqn (4)). This angle was calculated for two limit cases: (a) for initially aligned spins of main-sequence stars with the orbital angular momentum and (b) for a random initial misalignment of stellar spins. In the first case, nonzero angles θ_i prior to the coalescence can be expected only if some additional kick is imparted to the BH during the collapse (as in the case of neutron stars, see the discussion in [42]). For randomly misaligned initial spins of the binary components, the angle θ_i can be arbitrary (see [47] for more details).

2.3 Results of calculations

The results of population synthesis calculations of coalescing binary BHs taking the rotational evolution of cores of massive stars into account are presented in Fig. 1 (see the details of calculations and formulas in [47]). This figure shows the expected distribution of the effective spins $\chi_{\rm eff}$ of coalescing binary BHs that can be detected by LIGO/Virgo interferometers with the current O3 sensitivity [4] as a function of the total mass of the binary M (Fig. 1a, e) for the two BH formation models described above. The common envelope efficiency is assumed to be $\alpha_{\rm CE} = 1$. The initial spin axes of the binary components are assumed to be randomly misaligned. The grey gradient color shows the probability of the formation of coalescing binary BHs convolved with the metallicity and star formation rate evolution with look-back time (redshift) in galaxies. Squares with error bars show the parameters of the observed binary BHs from the O1/O2 catalogue [16]. The unfilled circles (shown in green online) represent additional BH + BH binaries reported from independent O1/O2 LIGO/Virgo data analysis [52]. The lighter symbols correspond to a higher probability of spurious (nonastrophysical) detections. It is seen that the results of the BH formation model without fallback (the upper panel) approximately describe the narrow distribution of the effective spins around zero (but for several less reliable sources found in [52]) (Fig. 1c), but do not encompass the most massive coalescing BHs (Fig. 1b). In the model of BH formation with fallback from the rotating envelope (Fig. 1e–h), the total masses of the coalescing binary BHs better correspond to observations, and the calculated effective spin distribution predicts the existence of rapidly rotating binary BHs (high values of $\chi_{\rm eff}$), which have not yet been reliably found. Clearly, the successful performance of the LIGO/Virgo detectors during the O3 run started in April 2019 will enable significant growth of the source statistics and a more accurate comparison with models.[5]

3. Spins of coalescing neutron star–black hole binaries

The widely recognized evolutionary model of massive binary stars [42] also predicts the formation of close binary systems containing neutron stars with black holes (BH + NS). The NS in such a binary observed as a radio pulsar would offer a unique probe of space–time around the companion BH by accurate pulsar timing measurements. Population synthesis calculations have predicted about one PSR + BH system for every several thousand single pulsars in the Galaxy [54], but searches for such binaries have failed so far. There is hope that such binaries can be first discovered by gravitational astronomy methods. The formation rate of BH + NS binaries is much lower than that of NS + NS and BH + BH binaries because the formation of the secondary (lighter) NS companion in a massive binary is accompanied by significant mass loss from the system and additional kick imparted to the NS during the supernova explosion, which in many cases can result in the disruption of the binary system (see, e.g., reviews [41, 42] for more details).

Figure 2 shows the calculated spatial density of binary BH + BH and BH + NS coalescences (per year per cubic Gpc) for the model assumptions as in [47] about the evolution of the stellar metallicity and star formation rate in the Universe depending on the redshift z. The common envelope efficiency varied in the range $0.5 \leqslant \alpha_{\rm CE} \leqslant 4$. The NS kick velocity is assumed to follow a Maxwellian distribution with the mean 256 km s^{-1}. It can be seen that the coalescence rate of BH + NS binaries per unit volume is at least an order of magnitude smaller than that of a binary BH + BH, which so far has not contradicted the observed LIGO/Virgo detection statistics.

Figure 3 presents the theoretically expected detection rate per year as a function of the limit redshift (the integrated coalescence rate per unit volume up to the distance corresponding to a given z). The solid lines show the detection rate of binary black hole (BH + BH) coalescences taking the star formation rate history into account for the common envelope efficiency parameter $\alpha_{\rm CE} = 1$. The dashed lines marked with 'BH + BH LIGO det' and 'NS + BH LIGO det' show the expected LIGO/Virgo O3 detection rate $\mathcal{R}_{\rm BHBH} \sim 2 \times 10^2$ yr^{-1} and $\mathcal{R}_{\rm BHNS} \sim 1$ yr^{-1} of BH + BH and BH + NS coalescences. The specific volume rates of BH + NS coalescences shown in Figs 2 and 3 are in agreement with independent calculations (see, e.g., [55]).

Figure 4 shows the effective spin distributions of coalescing NS + BH binaries Eqn (4), as a function of the total mass for two BH formation models (as in Fig. 1). The dimensionless NS spin is defined in the same way as for a BH: $a^*_{\rm NS} = J_{\rm NS}/M^2_{\rm NS}$, where $J = I\omega_{\rm NS} = 2\pi I/P_{\rm NS}$ is the NS

[4] In the ongoing O3 observations, the detection horizon of NS + NS binaries with a chirp mass of $1.2M_\odot$ averaged over the viewing angle is about 120 Mpc. The detection horizon for coalescing compact binaries depends on the chirp mass as $D_{\rm h} \sim \mathcal{M}^{5/6}$ [53].

[5] At the time of writing, about two dozen new BH + BH detections have been reported; see the list in https://gracedb.ligo.org/latest/. The parameters of these binaries will be reported after careful analysis only at the end of 2019.

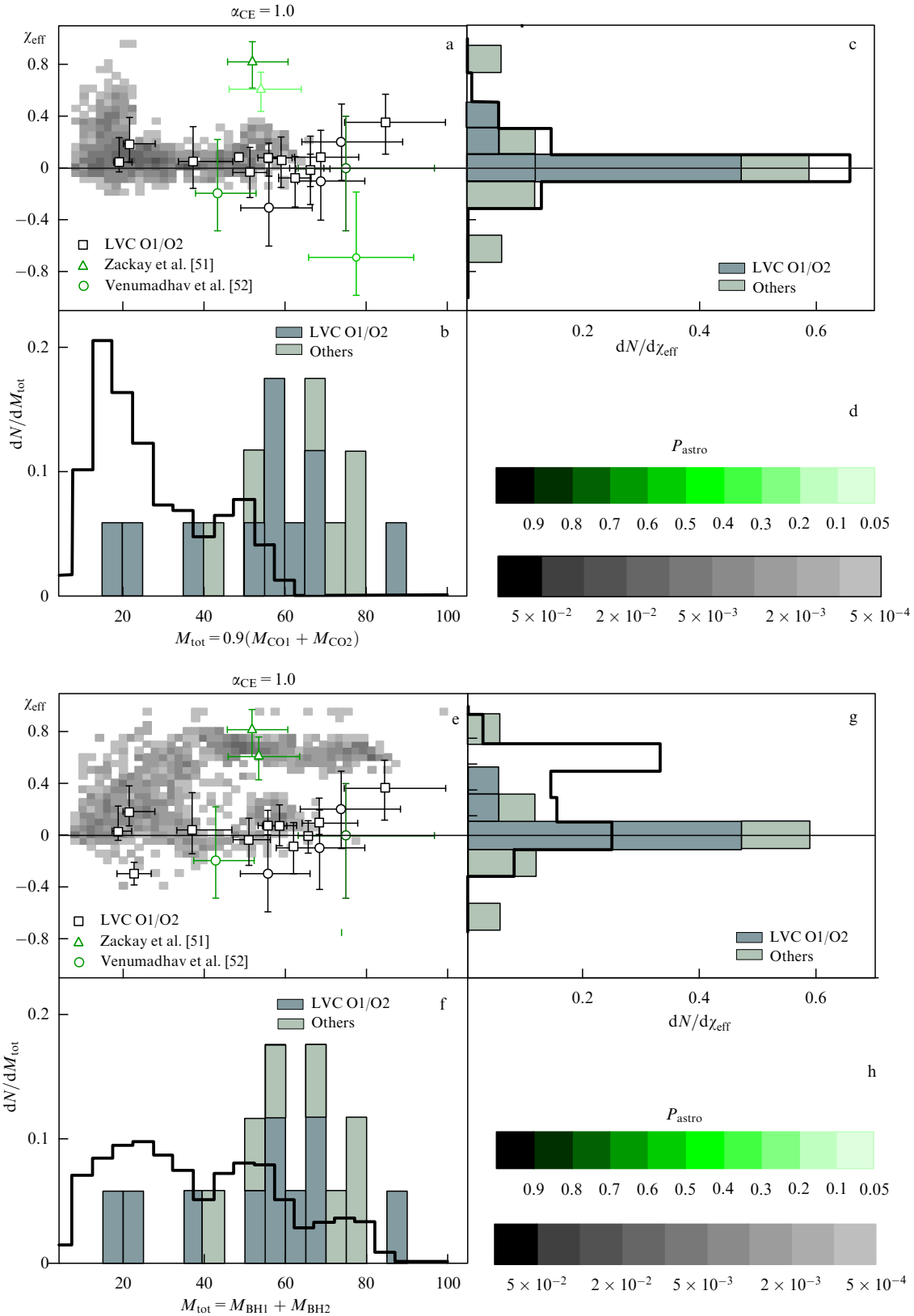

Figure 1. (Color online.) Model total mass M_{tot}–effective spin χ_{eff} distribution (normalized to unity) of coalescing binary BHs that can be detected at the current O3 LIGO/Virgo sensitivity calculated taking the star formation history in galaxies into account. The upper panels (a–d) shows the results for the direct collapse of the C–O stellar core into a BH (without fallback from the envelope): $M_{tot} = 0.9(M_{CO1} + M_{CO2})$. The bottom panels (e–h) show the model with a partial fallback of the envelope into the BH, with the BH mass as in [50]. The assumed common envelope efficiency is $\alpha_{CE} = 1.0$, the core–envelope coupling time is $\tau_c = 5 \times 10^5$ years. Shown are the events from the published O1/2 LIGO/Virgo Collaboration (LVC) Catalogue (the unfilled squares) as well as additional events from [51, 52] (unfilled triangles and circles). The color grade reflects the probability of their astrophysical origin P_{astro}.

angular momentum (I is the NS moment of inertia). The NS angular momentum was calculated taking the evolution of NS rotational period P_{NS} in a binary system into account (see [56] for more details). Generally, the effective spin distribu-

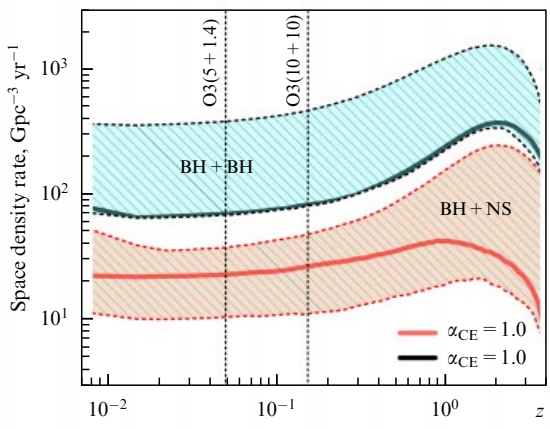

Figure 2. Spatial density of the coalescent rate of black hole–black hole (BH + BH) and neutron star–black hole (BH + NS) binaries (per year per cubic Gpc) as a function of the cosmological redshift z for a range of the common envelope efficiency parameter α_{CE} taking the star formation rate and stellar metallicity evolution in the Universe into account. The respective upper and lower boundaries of the hatched regions correspond to $\alpha_{CE} = 4.0$ and $\alpha_{CE} = 0.5$; the bold lines correspond to $\alpha_{CE} = 1.0$. The vertical dashed lines show the LIGO/Virgo O3 detection horizon for coalescing compact binaries with component masses $(5 + 1.4)M_\odot$ and $(10 + 10)M_\odot$.

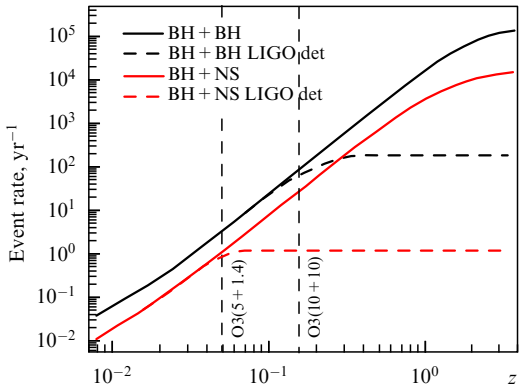

Figure 3. (Color online.) Expected event rate per year of compact binary coalescences (integrated space density rate up to distances corresponding to a given redshift z) as a function of the limit redshift (the detection horizon). The rate is calculated taking the star formation and stellar metallicity evolution in the Universe into account and for the assumed common envelope efficiency parameter $\alpha_{CE} = 1$. The respective thick black and red curves correspond to BH + BH and BH + NS coalescences. The dashed curves show the expected number of LIGO/Virgo O3 detections for the average orbit viewing angles $\mathcal{R}_{BHBH} \sim 2 \times 10^2$ yr^{-1} and $\mathcal{R}_{BHNS} \sim 1$ yr^{-1} for BH + BH and BH + NS events. The vertical dashed lines show the O3 LIGO/Virgo detection horizon for binaries with masses $(5 + 1.4)M_\odot$ and $(10 + 10)M_\odot$.

tion of coalescing NS + BH binaries for different BH formation models is symmetric around the zero value but broader than that for a binary BH + BH (see Fig. 1). Negative values of χ_{eff} for NS + BH binaries are due to the randomly directed NS kick velocity. The total mass of the coalescing NS + BH binaries in these calculations does not exceed $27\,M_\odot$.

4. Spins of coalescing primordial black holes

Near-zero effective spins of the coalescing binary BHs detected by LIGO/Virgo can be related to their origin and evolution and are widely discussed in the literature (see, e.g., [47, 58–62] and the references therein). As shown in Section 3, the narrow distribution of the effective spins of the observed coalescing binary BHs near zero can be reproduced in the standard astrophysical channel of the binary BH formation from massive binary systems [43], assuming no additional fallback from the rotating stellar envelope (model 1 in Section 2; see Fig. 1a–d). In addition to astrophysical scenarios of binary BH formation [63], in which $(10-50)M_\odot$ BHs result from core collapses of massive stars, the possibility of the existence of primordial binary BHs originating in the early Universe from primordial cosmological perturbations has been actively discussed [64–68]. The spins of primordial BHs should be nearly zero [69, 70] and hence the effective spin of coalescing primordial binary BHs is expected to be small.

To check the last statement, in [57] we studied the possibility of accretion spin-up of BH components of a primordial binary BH in an external medium. An initially nonrotating BH acquiring the mass $\Delta M = M_f - M_0$ from the ambient medium through an accretion disc, where M_0 and M_f are the initial and final masses of the BH, acquires the spin [7]

$$a^* = \sqrt{\frac{2}{3}}\left(\frac{M_0}{M_f}\right)\left[4 - \sqrt{18\left(\frac{M_0}{M_f}\right)^2 - 2}\right] \qquad (6)$$

(if no angular momentum is taken away by the disc radiation; the formula is valid for $M_f/M_0 < \sqrt{6}$; otherwise, $a^* = a^*_{max} \simeq 0.998$, the so-called Thorne limit [8]). For $\Delta M \ll M_0$ we obtain the estimate $a^* \simeq 9/\sqrt{6}\,(\Delta M/M_0)$ from (6).

For a single BH with a mass m moving with a velocity v, the fractional mass increase due to the Bondi–Hoyle–Lyttleton accretion over time t_0 is

$$\frac{\Delta M}{M_0} \approx \frac{4\pi\rho m}{(v^2 + c_s^2)^{3/2}}\,t_0\,, \qquad (7)$$

where ρ is the medium density and $c_s \sim \sqrt{T} \approx 10^{-5}\sqrt{T/1\text{ eV}}$ is the sound velocity in the medium with a temperature T. For a $1\,M_\odot$ BH in a medium with the density $\rho \sim 10^{-24}$ g cm^{-3} under the condition $v \gg c_s$ over the Hubble time $t_0 = t_H = 4 \times 10^{17}$ s, we obtain $\Delta M/M_0 \simeq 1.7 \times 10^{-3} m \ll 1$. Thus, the possible accretion-induced spin acquired by a single BH is $a^* \simeq 3.76\Delta M/M_0 \simeq 0.006(m/M_\odot)$. For a BH with the mass $m = (30-50)M_\odot$, the spin can be noticeable, but it is very difficult to measure the spin of a single BH.

In a binary system, the effective BH spin can be measured from gravitational-wave observations. Integration of the accreting mass from the ambient medium over the orbit in the binary BH system [57] shows that for two point-like masses m_1 and m_2 (with $q = m_1/m_2$ being the binary mass ratio and $M = m_1 + m_2 = m_1(1 + 1/q)$ the total mass) the accretion-induced fractional mass growth of the mass M_1 over the Hubble time t_H is

$$\left.\frac{\Delta M_1}{M_1}\right|_0 = \frac{5\pi\rho M^{1/2} a_0^{11/2}}{88 m_2^4} = \frac{5}{88}\left(\frac{256}{5}\right)^{11/8} \pi\rho t_H^{11/8} m_1^{5/8} q^{3/4}(1+q)^{15/8}\,. \qquad (8)$$

Here, the well-known relation between the coalescence time of a binary due to GW emission with the initial orbital semi-major axis a_0 is used: $t_0 = 5a_0^4/(256 M m_1 m_2)$. Numerically, for $m_1 = 30M_\odot$, we obtain a very low value, $\Delta M_1/M_1 \sim 10^{-6} - 10^{-7}$.

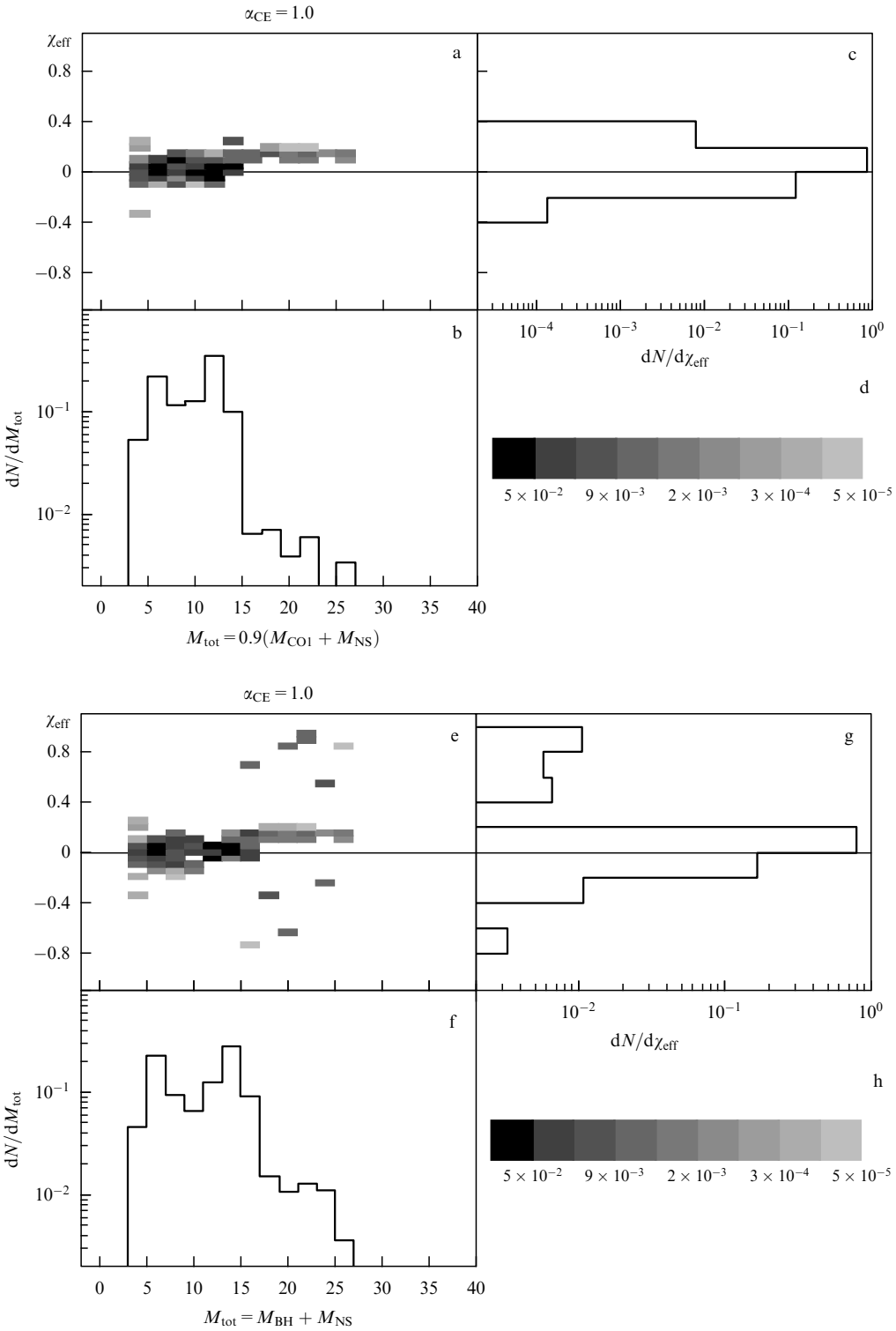

Figure 4. Model effective spin and total mass distributions for coalescing BH + NS binaries. The BH formation parameters are the same as for the BH + BH binaries in Fig. 1.

However, the estimate of the accretion-induced BH mass growth in a binary system significantly increases if the initial orbit is highly eccentric, $e_0 \sim 1$. In this case [57],

$$\left.\frac{\Delta M_1}{M_1}\right|_e \approx 10^{-5}\left(\frac{\rho}{10^{-24}\ \mathrm{g\ cm^{-3}}}\right)\left(\frac{M_1}{30M_\odot}\right)^{5/8} \times q^{3/4}(1+q)^{15/8}\left(\frac{0.1}{1-e_0^2}\right)^{2.58}$$

$$\approx 10^{-5}\left(\frac{\rho}{10^{-24}\ \mathrm{g\ cm^{-3}}}\right)\left(\frac{\mathcal{M}}{30M_\odot}\right)^{5/8} q(1+q)^2\left(\frac{0.1}{1-e_0^2}\right)^{2.58}. \quad (9)$$

In the last equation, the chirp mass of the binary system was introduced as $\mathcal{M} \equiv (M_1M_2)^{3/5}/M^{1/5} = M_1[q^2(1+q)]^{-1/5}$, which can be directly inferred from an analysis of spiraling GW waveforms from a coalescing binary consisting of two point-like masses.

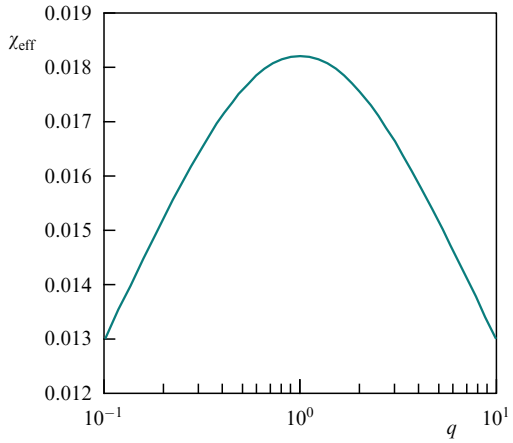

Figure 5. Maximum effective spin of a coalescing primordial binary BH with the chirp mass $\mathcal{M} = 30M_\odot$ acquired due to accretion in a medium with the sound velocity $c_s = 3$ km s^{-1} and density $\rho = 10^{-24}$ g cm^{-3} as a function of the binary component mass ratio q. (From [57].)

The effective spin of a primordial binary BH accreting from the external medium is found to be

$$\chi_{\rm eff} = \frac{q}{1+q}\,a_1^* + \frac{1}{1+q}\,a_2^* \approx 3.76\times10^{-5}\left(\frac{\rho}{10^{-24}\ {\rm g\ cm^{-3}}}\right) \times \left(\frac{\mathcal{M}}{30M_\odot}\right)^{5/8}\left(\frac{0.1}{1-e_0^2}\right)^{2.58}(1+q)(q^2+q^{-3}) > 5.3\times10^{-4}\left(\frac{\rho}{10^{-24}\ {\rm g\ cm^{-3}}}\right)\left(\frac{\mathcal{M}}{30M_\odot}\right)^{5/8}\left(\frac{0.1}{1-e_0^2}\right)^{2.58} \quad (10)$$

for any mass ratio f, because the function $f(q) = (1+q)(q^2+q^{-3})$ has the minimum $f(q_{\rm min}) = 4$ at $q_{\rm min} = 1$. Accounting for the constraint on the maximum possible value of the initial eccentricity for a given sound velocity of the external medium c_s leads to the maximum possible $\chi_{\rm eff}$ shown in Fig. 5. A rough upper bound can be written as

$$\chi_{\rm eff,\,max} \simeq 0.01\left(\frac{\rho}{10^{-24}\ {\rm g\ cm^{-3}}}\right)\left(\frac{\mathcal{M}}{30\,M_\odot}\right)^{0.97}\left(\frac{c_s}{10^{-5}}\right)^{-2.75}$$

in a wide mass ratio interval $0.1 < q < 10$. This estimate suggests that the effective spin of coalescing primordial binary BHs can be a few percent due to accretion of gas from the cold interstellar medium. In this spin-up mechanism, the spins of both BH components must be aligned with the binary orbital angular momentum.

5. Conclusions

Measurements of BH rotation from astronomical observations remain a relevant problem for modern astrophysics. The angular momentum (spin) of a BH is the second most important parameter (after the mass) determining the structure of space–time around the BH. The rotation of BHs in close X-ray binaries and in galactic nuclei is likely to be a necessary condition for launching relativistic jets in AGNs and microquasars and can determine the structure of the outflows (see review [71]). Gravitational-wave astronomy offered new possibilities of direct measurement of BH spins in coalescing binary BHs. The current LIGO/Virgo results [16] suggest a fairly narrow effective BH spin distribution around zero $\chi_{\rm eff}$, which can be used to understand the origin of coalescing binary BHs with masses of $(10-60)M_\odot$ [72, 73].

We have shown (see [47] and Fig. 2) that the astrophysical channel of coalescing binary BH formation from the evolution of massive binary stars taking the evolution of stellar metallicity and the star formation rate in the Universe into account leads to the effective BH spin and total mass of coalescing binary BH distribution that does not contradict the current LIGO/Virgo results [16]. Additional fallback of matter from the rotating stellar envelope onto a newborn BH resulting from a massive star iron core collapse can significantly spin up the BH, leading to a wide effective spin range (see Fig. 1e–h). The rapid rotation of components of coalescing binary BHs has not yet been reliably found [16], although there are indications that such binaries are present in the O1/O2 LIGO/Virgo data [51, 52]. These additional sources require confirmation.

Undiscovered up to now (June 2019) remain coalescing compact binaries hosting a black hole and a neutron star. The existence of such systems follows from the modern theory of evolution of massive binaries. Using the same model assumptions of BH formation, we have calculated the coalescence rates of NS + BH binaries (see Fig. 2) and their detection rate by the O3 LIGO/Virgo interferometers (see Fig. 3). For standard assumptions about the binary evolution parameters, the detection rate of BH + NS binaries is more than one order of magnitude lower than that of BH + BH binaries (see the dashed curves in Fig. 3): $\mathcal{R}_{\rm BHBH} \sim 2\times10^2$ yr^{-1} and $\mathcal{R}_{\rm BHNS} \sim 1$ yr^{-1}. The chances of detecting these types of coalescing compact binaries in the ongoing O3 LIGO/Virgo observations are not very high. We also calculated the expected distribution of the effective spins of BH + NS binaries depending on the assumed BH formation model (see Fig. 4). Due to the substantial kick velocity imparted to a newborn NS, the effective spins of NS + BH coalescing binaries fall within a wide range, $-0.4 < \chi_{\rm eff} < 0.4$, even in the conservative case without fallback of matter from the rotating stellar envelope onto the newborn BH (upper panel in Fig. 4a–d).

We have also considered the possible spin-up of primordial BHs due to gas accretion from the cold interstellar medium. We have shown (see [57] and Fig. 5) that the accretion spin-up of primordial BHs in binary systems can result in effective spins of the order of several percent; therefore, small positive effective spins of an observed coalescing BH + BH system does not contradict the hypothesis of their possible primordial origin.

Acknowledgements

The work of KAP is partially supported by the RSF grant no. 19-42-02004 (Sections 1.1–1.3, 4.2.2, and the general supervision). A G K and N A M acknowledge the support of the Scientific School of Lomonosov Moscow State University 'Physics of Stars, Relativistic Objects and Galaxies.'

Note added in proof. On August 14, 2019, the LIGO/Virgo detectors registered the coalescence of a compact binary highly likely consisting of an NS and a BH (S190814bv). No electromagnetic counterparts of this event have been reported so far.

References

1. Kerr R P *Phys. Rev. Lett.* **11** 237 (1963)
2. Boyer R H, Lindquist R W *J. Math. Phys.* **8** 265 (1967)

3. Wiltshire D L, Visser M, Scott S M *The Kerr Spacetime. Rotating Black Holes in General Relativity* (Cambridge: Cambridge Univ. Press, 2009)
4. Lense J, Thirring H *Phys. Z.* **19** 156 (1918)
5. Bardeen J M, Press W H, Teukolsky S A *Astrophys. J.* **178** 347 (1972)
6. Kaplan S A *Zh. Eksp. Teor. Fiz.* **19** 951 (1949)
7. Bardeen J M *Nature* **226** 64 (1970)
8. Thorne K S *Astrophys. J.* **191** 507 (1974)
9. Cherepashchuk A M *Phys. Usp.* **57** 359 (2014); *Usp. Fiz. Nauk* **184** 387 (2014)
10. Cherepashchuk A M *Phys. Usp.* **59** 702 (2016); *Usp. Fiz. Nauk* **186** 778 (2016)
11. Brumberg V A et al. *Sov. Astron. Lett.* **1** 2 (1975); *Pis'ma Astron. Zh.* **1** 5 (1975)
12. Rhoades C E (Jr.), Ruffini R *Phys. Rev. Lett.* **32** 324 (1974)
13. Lattimer J M, Prakash M *Phys. Rep.* **621** 127 (2016)
14. Remillard R A, McClintock J E *Annu. Rev. Astron. Astrophys.* **44** 49 (2006)
15. Abbott B P et al. (LIGO Scientific Collab., Virgo Collab.) *Phys. Rev. Lett.* **116** 061102 (2016)
16. Abbott B P et al. (LIGO Scientific Collab., Virgo Collab.) *Phys. Rev. X* **9** 031040 (2019)
17. Cherepashchuk A M *Phys. Usp.* **59** 910 (2016); *Usp. Fiz. Nauk* **186** 1001 (2016)
18. Reitze D H *Phys. Usp.* **60** 823 (2017); *Usp. Fiz. Nauk* **187** 884 (2017)
19. Shakura N I *Sov. Astron.* **16** 756 (1973); *Astron. Zh.* **49** 921 (1972)
20. Shakura N I, Sunyaev R A *Astron. Astrophys.* **24** 337 (1973)
21. Novikov I D, Thorne K S, in *Black Holes* (*Les Astres Occlus*) (Eds C DeWitt, B DeWitt) (New York: Gordon and Breach, 1973) p. 343
22. Zhuravlev V, in *Accretion Flows in Astrophysics* (Astrophysics and Space Science Library, Vol. 454, Ed. N Shakura) (Cham: Springer, 2018) p. 115
23. Nampalliwar S, Bambi C, arXiv:1810.07041
24. Reynolds C S *Nature Astron.* **3** 41 (2019)
25. Laor A *Nature Astron.* **3** 374 (2019)
26. George I M, Fabian A C *Mon. Not. R. Astron. Soc.* **249** 352 (1991)
27. Laor A *Astrophys. J.* **376** 90 (1991)
28. Tanaka Y et al. *Nature* **375** 659 (1995)
29. Fabian A C et al. *Nature* **459** 540 (2009)
30. van der Klis M, astro-ph/0410551
31. Stella L, Vietri M, Morsink S M *Astrophys. J.* **524** L63 (1999)
32. Abramowicz M A, Kluźniak W *Astron. Astrophys.* **374** L19 (2001)
33. Motta S E et al. *Mon. Not. R. Astron. Soc.* **437** 2554 (2014)
34. Motta S E et al. *Mon. Not. R. Astron. Soc.* **439** L65 (2014)
35. Shaposhnikov N, Titarchuk L *Astrophys. J.* **699** 453 (2009)
36. Akiyama K et al. (The Event Horizon Telescope Collab.) *Astrophys. J. Lett.* **875** L1 (2019)
37. Akiyama K et al. (The Event Horizon Telescope Collab.) *Astrophys. J. Lett.* **875** L5 (2019)
38. Tamburini F, Thidé B, Della Valle M *Mon. Not. R. Astron. Soc.* **492** L22 (2020)
39. Meynet G, Maeder A, in *Handbook of Supernovae* (Eds A W Alsabti, P Murdin) (Cham: Springer, 2017) p. 601
40. Woosley S E, Bloom J S *Annu. Rev. Astron. Astrophys.* **44** 507 (2006)
41. Grishchuk L P et al. *Phys. Usp.* **44** 1 (2001); *Usp. Fiz. Nauk* **171** 3 (2001)
42. Postnov K A, Yungelson L R *Living Rev. Relativ.* **17** 3 (2014)
43. Belczynski K et al. *Nature* **534** 512 (2016)
44. Spruit H C *Astron. Astrophys.* **381** 923 (2002)
45. Fuller J et al. *Astrophys. J.* **810** 101 (2015)
46. Postnov K A et al. *Mon. Not. R. Astron. Soc.* **463** 1642 (2016)
47. Postnov K A, Kuranov A G *Mon. Not. R. Astron. Soc.* **483** 3288 (2019)
48. Webbink R F *Astrophys. J.* **277** 355 (1984)
49. Iben I (Jr.), Tutukov A V *Astrophys. J. Suppl.* **54** 335 (1984)
50. Fryer C L et al. *Astrophys. J.* **749** 91 (2012)
51. Zackay B et al. *Phys. Rev. D* **100** 023007 (2019)
52. Venumadhav T et al., arXiv:1904.07214
53. Abadie J et al. (LIGO Scientific Collab., Virgo Collab.), LIGO-T0900499-v19; VIR-0171A-10; arXiv:1003.2481
54. Lipunov V M et al. *Astrophys. J.* **423** L121 (1994)
55. Baibhav V et al. *Phys. Rev. D* **100** 064060 (2019)
56. Lipunov V M et al. *Astron. Rep.* **53** 915 (2009); *Astron. Zh.* **86** 985 (2009)
57. Postnov K, Mitichkin N A *J. Cosmol. Astropart. Phys.* **2019** (06) 044 (2019)
58. Belczynski K et al. *Astron. Astrophys.* **615** A91 (2018)
59. Talbot C, Thrane E *Phys. Rev. D* **96** 023012 (2017)
60. Ng K K Y et al. *Phys. Rev. D* **98** 083007 (2018)
61. Piran T, Hotokezaka K, arXiv:1807.01336
62. Fernandez N, Profumo S *J. Cosmol. Astropart. Phys.* **2019** (08) 022 (2019)
63. Mandel I, Farmer A, arXiv:1806.05820
64. Nakamura T et al. *Astrophys. J.* **487** L139 (1997)
65. Bird S et al. *Phys. Rev. Lett.* **116** 201301 (2016)
66. Carr B, Kühnel F, Sandstad M *Phys. Rev. D* **94** 083504 (2016)
67. Blinnikov S et al. *J. Cosmol. Astropart. Phys.* **2016** (11) 036 (2016)
68. Sasaki M et al. *Phys. Rev. Lett.* **117** 061101 (2016)
69. Mirbabayi M, Gruzinov A, Noreña J, arXiv:1901.05963
70. De Luca V et al. *J. Cosmol. Astropart. Phys.* **2019** (05) 018 (2019)
71. Beskin V S *Phys. Usp.* **53** 1199 (2010); *Usp. Fiz. Nauk* **180** 1241 (2010)
72. Tiwari V, Fairhurst S, Hannam M *Astrophys. J.* **868** 140 (2018)
73. Gerosa D et al. *Phys. Rev. D* **98** 084036 (2018)